Flow-induced arrest of spatiotemporal chaos and transition to a stationary pattern in the Gray-Scott model

Debojyoti Das*

Indian Association for the Cultivation of Science, Jadavpur, Kolkata 700 032, India

(Received 25 June 2015; revised manuscript received 7 October 2015; published 30 November 2015)

We examine the prototypical Gray-Scott model, which mimics cubic autocatalytic reaction with linear decay of the autocatalyst, to model the kinetics of a reaction-diffusion system subjected to advective streamline flow. For a proper choice of boundary conditions and parameter space, the system admits wave-induced spatiotemporal chaos in the absence of flow. We show that flow above a critical value leads to an arrest of the spatiotemporal chaos due to a change in the instability from absolute to convective type. Furthermore, stationary spatial structures are borne out of a second successive bifurcation for yet another critical flow value. The theoretical formulations are corroborated by extensive numerical simulation of the full reaction-diffusion-advection system in one dimension.

DOI: 10.1103/PhysRevE.92.052914 PACS number(s): 05.45.Ac, 47.20.−k, 89.75.Kd

I. INTRODUCTION

Temporal and spatial self-organization is ubiquitous in systems open to exchange of mass and/or energy with the surroundings. Although dissipative structures are observed in both zero-dimensional and spatially extended systems encompassing a rich variety of interesting physics [1,2], the plethora of novel dynamical scenarios that the latter provides over the former is manifold due to the involvement of the spatial degrees of freedom. The two most well studied routes to spatial structures in activator-inhibitor systems are differential diffusivity of participating species leading to a Turing pattern [3], and differential flow of the reactants leading to a traveling-wave-type pattern [4]. A third mechanism capable of producing spatial patterns involves equal diffusivities and flow rates for a system that exhibits autonomous oscillations for homogeneous conditions in the absence of flow [5,6]. Among the spatiotemporal structures that develop, perhaps the most intriguing and least understood is spatiotemporal chaos.

In the zero-dimensional systems the possible routes to chaos are the Ruelle-Takens-Newhouse scenario (three successive Hopf bifurcations), Feigenbaum (infinite sequence of period doubling bifurcations), and Pomeau-Manneville scenario (saddle-node bifurcation), with a minimum requirement of three variables (necessary but not sufficient) [7]. However, in case the system has spatial extension, spatiotemporal chaos can occur even in a two-variable model. Spatiotemporal chaos has been realized in numerous studies on reaction-diffusion systems [8–16]. Systems with spatiotemporal chaos are characterized by rapid decay of the spatial correlation function, sensitivity to initial conditions [16], and at least one positive Lyapunov exponent [17,18]. However, it has been shown by Wackerbauer and Showalter [10] that for no-flux and periodic boundary conditions, the Gray-Scott model ceases to exhibit spatiotemporal chaos in the asymptotic limit, although the average transient lifetime increases exponentially with the size of the system.

Nonetheless, sustained spatiotemporal chaos is obtained by imposing a constant value boundary (Dirichlet boundary) at one end which acts as a source of continuous perturbations and precludes the possible return to the homogeneous steady state. Although such a contraption was originally meant to obtain stationary space-periodic structures in systems with equal diffusion coefficients [6], it comes at a cost of producing sustained spatiotemporal chaos, e.g., in the spatially extended Gray-Scott system. Suppression of spatiotemporal chaos [19,20] has been affected by some methods involving delay, such as global delayed feedback [19] and time-delay autosynchronization [20].

In the present paper we consider the two-variable Gray-Scott model in one dimension that serves as a paradigm for open, autocatalytic reaction systems. Additionally, with the advent of chemical reactors that admit sustained pattern formation, the possibility to explore novel dynamical scenarios has opened up. For example, the Couette reactor [21–23], which is effectively a one-dimensional system having well-defined boundary conditions and controlled diffusion coefficient (having the same value for all the participating species, identical to the scenario presented in this study), might serve as a possible setup to test our theory experimentally, provided the setup can accommodate advection. For the system of our interest, the Gray-Scott model, a proper choice of parameters together with a constant boundary at one end and a zero-flux boundary (Neumann boundary) at the other end, we obtain sustained spatiotemporal chaos that is marked by rapid loss of spatial correlation, extreme sensitivity to initial conditions, and a positive Lyapunov exponent [17,18]. By switching on a constant streamline flow, we not only eliminate spatiotemporal chaos but also retrieve stationary spatial structures by the same mechanism that stabilizes stationary pattern structures by the successive occurrence of absolute and convective instabilities [24]. To this end the present study can be envisaged as a physically plausible prescription to select spatiotemporal regimes of interest solely by the control of flow strength.

The outline of the paper is as follows: In Sec. II we describe the reaction-diffusion-advection model for a system with Gray-Scott kinetics. In the subsequent section (Sec. III) we carry out linear stability analysis to derive conditions for the crossover from absolute to convective instability, followed by development of stationary patterns. The theoretical predictions formulated on the one-dimensional Gray-Scott model are corroborated by the results of the numerical simulations in Sec. IV. The paper is concluded in Sec. V.

*debojyotidas007@gmail.com

II. REACTION-DIFFUSION-ADVECTION MODEL: GOVERNING EQUATIONS

We consider the Gray-Scott reaction [25], i.e., a cubic autocatalytic reaction with linear decay of the autocatalyst, to model the kinetics of a reaction-diffusion-advection system. The corresponding dimensionless mass-balance equations for the open flow system in one dimension is represented by

$$\frac{\partial \alpha}{\partial t} + \sigma \frac{\partial \alpha}{\partial x} = 1 - \alpha - \mu\alpha\beta^2 + D_\alpha \frac{\partial^2 \alpha}{\partial x^2}, \qquad (2.1)$$

$$\frac{\partial \beta}{\partial t} + \sigma \frac{\partial \beta}{\partial x} = \beta_0 - \phi\beta + \mu\alpha\beta^2 + D_\beta \frac{\partial^2 \beta}{\partial x^2}, \qquad (2.2)$$

where the dimensionless concentration variables are α and β, and the dimensionless kinetic parameters are given by β_0, μ, and ϕ. Also, σ denotes the dimensionless flow rate of the intermediates, and the dimensionless diffusion coefficients of α and β are given by D_α and D_β, respectively. In this study we consider the case where $D_\alpha = D_\beta = D$.

A. Temporal dynamics

In the present paper we consider the special case wherein β is absent in the inflow stream, i.e., $\beta_0 = 0$. This special case provides certain analytical advantages, as now one steady state corresponds to the "no-conversion" state ($\alpha_{ss}^n = 1, \beta_{ss}^n = 0$), and the remaining steady states are given by ${\alpha_{ss}}^{\pm} = \frac{\mu \mp \sqrt{\mu^2 - 4\mu\phi^2}}{2\mu}$, ${\beta_{ss}}^{\pm} = \frac{\mu \pm \sqrt{\mu^2 - 4\mu\phi^2}}{2\mu\phi}$. Thus, the condition for existence of multiple steady states for the homogeneous Gray-Scott kinetics is $\mu > \mu_{sn} = 4\phi^2$, where μ_{sn} denotes the saddle-node bifurcation. Of these, the lowest root (a_{ss}^n, β_{ss}^n) is always a stable node (S_n), the middle root (a_{ss}^-, β_{ss}^-) is a saddle point (S_s), and the highest root (a_{ss}^+, β_{ss}^+) is a focus (S_f), which is stable for $\mu > \mu_H$, where $\mu_H = \frac{\phi^4}{\phi - 1}$ denotes the Hopf bifurcation line. The focus loses stability due to a Hopf bifurcation. The resulting limit cycle is unstable in the case where the Hopf bifurcation mode is subcritical, whereas a stable limit cycle occurs when the Hopf bifurcation mode is supercritical. The phase-space diagrams for the system with a stable node as the only attractor are shown in Fig. 1.

B. Spatiotemporal dynamics ($\sigma = 0$)

The spatially extended Gray-Scott model admits a variety of dissipative structures in the form of traveling waves, spirals, and target patterns. Traveling waves relevant to the present study are the simple pulse and the front. The former connects the stable node (S_n) in front to the same state behind the wave (homoclinic connections in the α-β phase plane), whereas the latter connects the stable node to the focus (heteroclinic connections in the phase plane). Two different situations arise, depending on the local (temporal) stability of the focus. In the case where the focus is stable, the system stays in the vicinity of this state as against the "no-conversion" state. The front carries the signature of the focus in the form of a damped oscillatory spatial distribution in its rear end. An unstable focus, on the other hand, changes the scenario rather curiously; considering temporal dynamics alone it is expected that the system would be forced to the stable node, the only stable

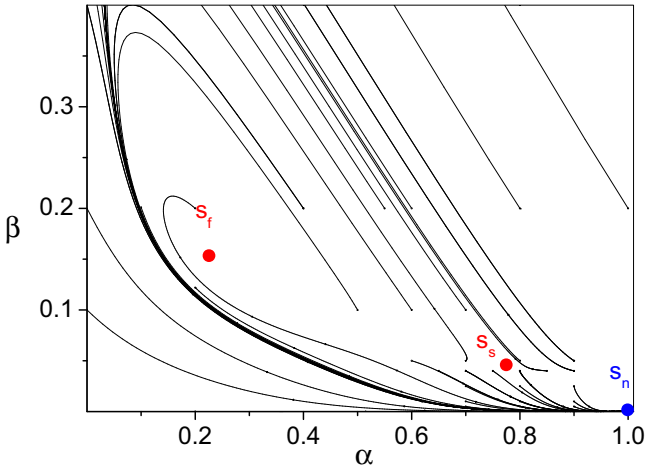

FIG. 1. (Color online) Phase-space diagram for the Gray-Scott model showing a stable node as the only attractor ($\mu = 155.0, \phi = 5.2$).

attractor in the system. However, due to the spatial extension of the system, even when a particular region returns to the stable node, its adjacent region, having nonzero concentration of the autocatalyst due to the recent passage of a front, can initiate a reaction front into the newly formed stable node. Repetition of this mechanism at different space points gives rise to a sustained spatiotemporal dynamics comprised of spatial evolution of the system to the vicinity of the stable node followed by reinjection of the system to the neighborhood of the unstable focus by propagation of reaction-diffusion fronts. This mechanism can result in wave-induced spatiotemporal chaos [8] for some parameter sets. For a more detailed description we refer to Merkin *et al.* [8,9].

III. STABILITY ANALYSIS: BIFURCATION CONDITIONS

We start our analysis using Eqs. (2.1) and (2.2) and linearize them about the focus (S_f) by introducing perturbations (A, B) given by $\alpha = \alpha_{ss}^+ + A$ and $\beta = \beta_{ss}^+ + B$. Here it is important to note that we do not consider the remaining steady states, since their stability properties preclude the possibility of spatiotemporal chaos, the pivotal point of this study. The resulting linearized equations are given by

$$\frac{\partial A}{\partial t} + \sigma \frac{\partial A}{\partial x} = D \frac{\partial^2 A}{\partial x^2} + J_{11} A + J_{12} B, \qquad (3.1)$$

$$\frac{\partial B}{\partial t} + \sigma \frac{\partial B}{\partial x} = D \frac{\partial^2 B}{\partial x^2} + J_{21} A + J_{22} B, \qquad (3.2)$$

where $J_{ij}, (i, j = 1,2)$ are elements of the Jacobian matrix J determined at the steady state $(\alpha_{ss}^+, \beta_{ss}^+)$,

$$J = \begin{bmatrix} J_{11} & J_{12} \\ J_{21} & J_{22} \end{bmatrix} = \begin{bmatrix} -(1 + \mu {\beta_{ss}}^2) & -2\mu\alpha_{ss}\beta_{ss} \\ \mu {\beta_{ss}}^2 & 2\mu\alpha_{ss}\beta_{ss} - \phi \end{bmatrix}. \qquad (3.3)$$

We assume solutions to Eqs. (3.1) and (3.2) to be of the form given by

$$A = \tilde{A} \exp[i(\kappa x - \lambda t)]; \quad B = \tilde{B} \exp[i(\kappa x - \lambda t)], \qquad (3.4)$$

where $\tilde{A}$, $\tilde{B}$ are constants, κ is the wave number, and λ is the growth rate of the perturbation. Substituting these trial solutions in Eqs. (3.1) and (3.2), we get

$$[-i\lambda + i\kappa\sigma + \kappa^2 D - J_{11}]\tilde{A} - J_{12}\tilde{B} = 0, \quad (3.5)$$

$$J_{21}\tilde{A} - [-i\lambda + i\kappa\sigma + \kappa^2 D - J_{22}]\tilde{B} = 0. \quad (3.6)$$

Nontrivial solutions of $\tilde{A}$ and $\tilde{B}$ are obtained by setting $\det|M - \lambda I| = 0$, where

$$M = \begin{bmatrix} M_{11} & M_{12} \\ M_{21} & M_{22} \end{bmatrix} = \begin{bmatrix} -i\lambda + i\kappa\sigma + \kappa^2 D - J_{11} & -J_{12} \\ J_{21} & -i\lambda + i\kappa\sigma + \kappa^2 D - J_{22} \end{bmatrix}.$$

The resulting dispersion relation is given by

$$\mathcal{D}(\lambda,\kappa) \equiv \lambda^2 + \{[2D\kappa^2 - \tau]i - 2\kappa\sigma\}\lambda - D^2\kappa^4 - 2iD\sigma\kappa^3 + [\sigma^2 + D\tau]\kappa^2 + i\sigma\tau\kappa - \Delta = 0, \quad (3.7)$$

where $\tau = J_{11} + J_{22}$ and $\Delta = J_{11}J_{22} - J_{12}J_{21}$ are the trace and determinant of the Jacobian matrix J, respectively. The fate of the steady state (focus in this case) is determined by the sign of the real part of the eigenvalue [Re (λ)].

A. Effect of flow: Transition from absolute to convective instability

Absolute instability corresponds to the situation wherein perturbations drive the system away from the initial state, resulting in the growth of amplitudes at all fixed points in space, which transforms the system to a state different from the steady state. On the other hand, convective instability corresponds to the situation where perturbations lift the system away from the steady state in the form of a wave that propagates with increase in size. However, in contrast to absolute instability, after passage of the wave front the system returns to the original steady state, meaning that an amplitude at a fixed point decays asymptotically towards zero [26,27]. The transition from the absolute to the convective instability occurs at a critical value of the dimensionless flow velocity, denoted by σ_{AC}. To derive the bifurcation curve, we start with the solution of Eq. (3.7), which is given by

$$\lambda(\kappa) = \tfrac{1}{2}(2\kappa\sigma - i[2D\kappa^2 - \tau] \pm \sqrt{4\Delta - \tau^2}). \quad (3.8)$$

Next we determine the group velocity by differentiating this with respect to κ and setting it equal to zero for $\kappa = \kappa_0$, i.e.,

$$\left.\frac{\partial\lambda(\kappa)}{\partial\kappa}\right|_{\kappa=\kappa_0} = 0. \quad (3.9)$$

The resulting $\kappa_0 = -\frac{i\sigma}{2D}$ is substituted back in Eq. (3.9) to give

$$\lambda(\kappa_0) = \frac{1}{2}\left[i\left(\tau - \frac{\sigma^2}{2D}\right) \pm \sqrt{4\Delta - \tau^2}\right]. \quad (3.10)$$

The condition for the transition from absolute to convective instability corresponds to the situation wherein the real part governing the time dependence of the trial solution in Eq. (3.4) becomes zero, i.e., $\mathrm{Im}[\lambda(\kappa_0)] = 0$. Provided $4\Delta - \tau^2 > 0$, the expression for the critical value of the dimensionless velocity (σ) to affect such a change is given by

$$\sigma_{AC} = \sqrt{2D\tau}. \quad (3.11)$$

The locus of the critical velocity for transition from absolute to convective instability σ_{AC} for the Gray-Scott model is shown in Fig. 2.

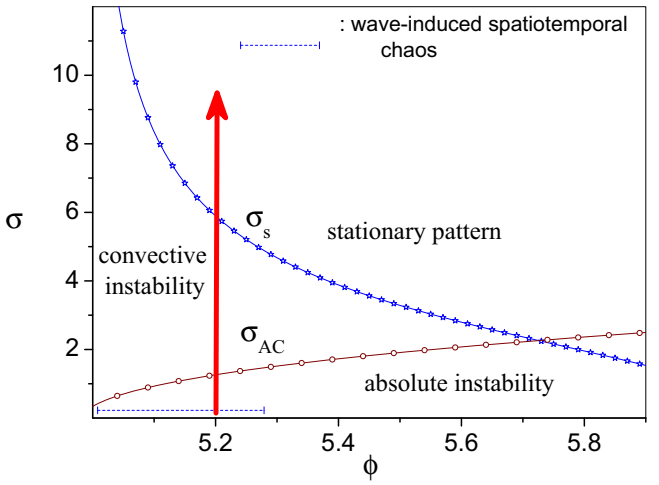

FIG. 2. (Color online) Bifurcation diagram showing regions of absolute instability, convective instability, and stationary pattern depending on the dimensionless flow σ. The region of wave-induced spatiotemporal chaos is denoted by blue dashed line. The solid (red) arrow depicts the transition to different regions in the bifurcation diagram as the critical flow values, given by σ_{AC} (line with unfilled circle) and σ_s (line with unfilled star), respectively, are crossed ($\mu = 155.0$).

B. Effect of flow: Transition to a stationary pattern

In mathematical terms a stationary pattern corresponds to setting the temporal growth rate equal to zero, i.e., $\lambda = 0$, together with $\mathrm{Im}(\kappa) = 0$. Physically this situation is equivalent to concentrations being stationary in time but periodic in space due to the presence of purely exponential perturbations ($\exp[i\kappa x]$). To this end, by setting $\lambda = 0$ in Eq. (3.7), we get

$$D^2\kappa^4 + 2iD\sigma\kappa^3 - (\sigma^2 + D\tau)\kappa^2 - i\sigma\tau\kappa + \Delta = 0. \quad (3.12)$$

The critical wave number (κ_s) that can accommodate stationary patterns is obtained by setting the coefficients of the imaginary part of the above equation equal to zero. The explicit expression for the critical wave number is given by

$$\kappa_s = \sqrt{\frac{\tau}{2D}}. \quad (3.13)$$

Substitution of this result in Eq. (3.13), then, gives the critical flow velocity for the transition to a stationary pattern:

$$\sigma_s = \sqrt{\frac{D(4\Delta - \tau^2)}{2\tau}}. \quad (3.14)$$

The bifurcation curve corresponding to the critical velocity (σ_s) needed to obtain a stationary pattern for the Gray-Scott model is depicted in Fig. 2.

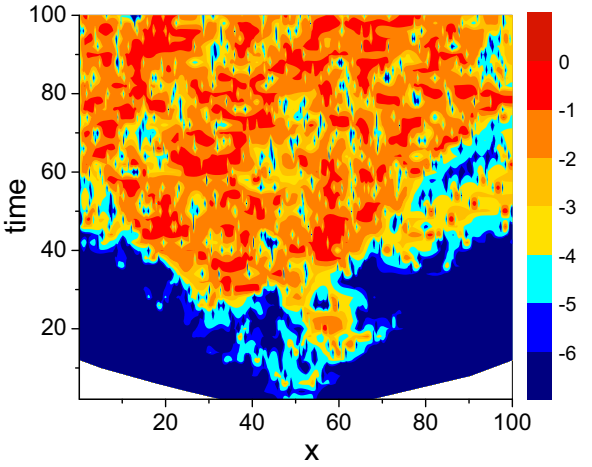

FIG. 3. (Color online) Initial condition sensitivity. Space-time plot of the absolute difference in α for two systems. The color coding represents the absolute difference between the two systems on a logarithmic scale from dark (blue) color (low difference) to light (red) color (high difference) with the same set of parameters ($\mu = 155, \phi = 5.20$) but differing in initial condition at a single point ($\tilde{x} = \frac{L}{2}$).

IV. RESULTS: NUMERICAL SIMULATIONS

In this section we verify the theoretical results of linear stability analysis obtained in the preceding section. To this end, we carried out extensive numerical integration of the reaction-diffusion-advection model in both the presence and absence of flow. For numerical integration of the partial differential equations [Eqs. (2.1) and (2.2)], we first discretized the spatial domain with grid spacing $dx = 0.10$ and then employed an explicit Euler method with a time increment of $dt = 0.001$. A Dirichlet (constant value) boundary is imposed at the inlet on the left $[(\alpha,\beta) = (0.25,0)]$, which acts as a pacemaker, while a Neumann (zero-flux) boundary is imposed at the outlet on the right.

A. Spatiotemporal dynamics: In absence of flow ($\sigma = 0$)

For the parameter set $\mu = 155, \phi = 5.2$ the Gray-Scott model has three steady states since $\mu > \mu_{sn}$. However, the system for the given set of parameters has only one stable attractor in the form of stable node (s_n). The absence of flow ($\sigma = 0$) and the constant boundary values of the participating species at the inlet give rise to spatiotemporal chaos by the mechanism described in Sec. II B. Nevertheless, to proceed

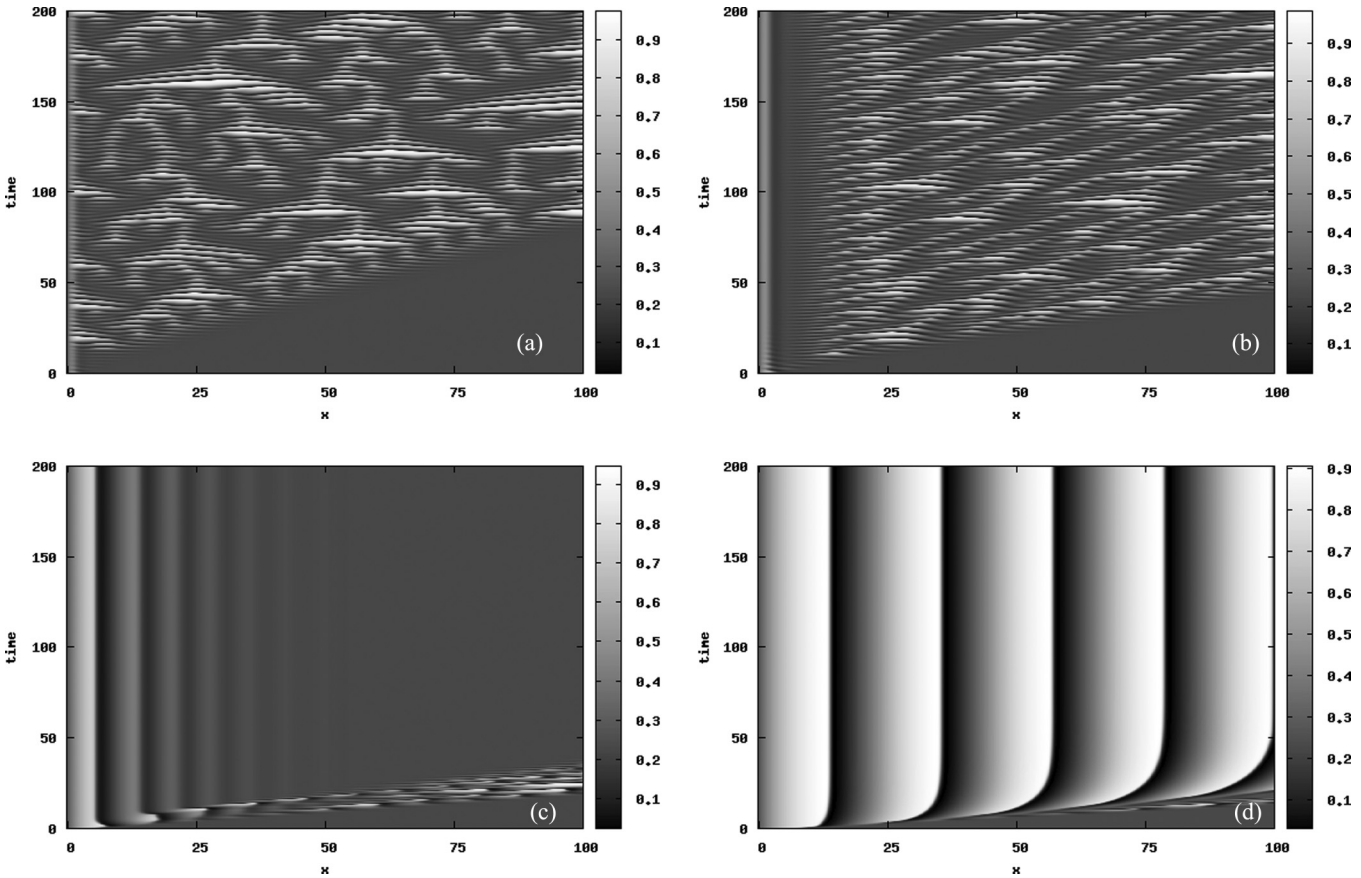

FIG. 4. Space-time plot of the spatiotemporal α variable for different values of flow pertaining to different zones of the bifurcation diagram (Fig. 2): (a) absolute instability region ($\sigma = 0.0$), (b) absolute instability region ($\sigma < \sigma_{AC}$), (c) convective instability region ($\sigma_{AC} < \sigma < \sigma_s$), and (d) stationary pattern region ($\sigma > \sigma_s$). Black color and white color correspond to low and high concentrations of the spatiotemporal α variable, respectively. System parameters: $\mu = 155, \phi = 5.20$.

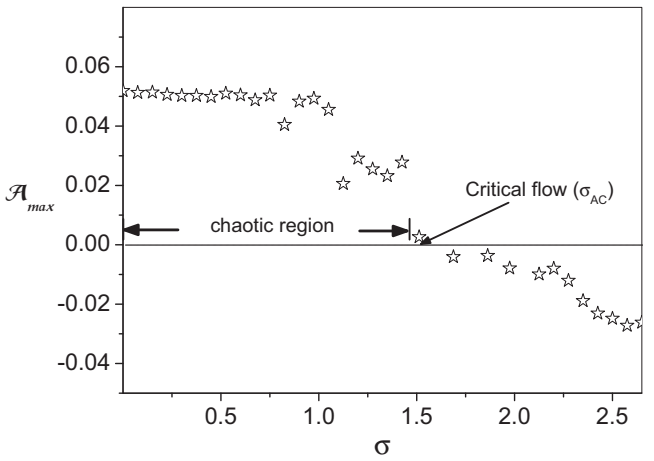

FIG. 5. The largest Lyapunov exponent ($\mathcal{A}_{\max}$) as a function of dimensionless flow σ. Parameter set used $\mu = 155$ and $\phi = 5.20$.

further the genuineness of the spatiotemporal chaos needs to be ascertained, although there seems to be no consensus on the conditions that must be satisfied for qualification of a spatiotemporal behavior as chaotic. Loss of spatial correlation, extreme sensitivity to initial conditions, and a positive value of the Lyapunov exponent ($\mathcal{A}$) [10,17,18] are well-accepted criteria for spatiotemporal chaos. The extreme sensitivity of the system to initial conditions for the same set of parameters characterizing spatiotemporal chaos is shown in Fig. 3. Next we define the spatial correlation function:

$$C(x-\tilde{x};t-\tilde{t}) = \langle[\alpha(x,t)-\langle\alpha\rangle][\alpha(\tilde{x},\tilde{t})-\langle\alpha\rangle]\rangle, \quad (4.1)$$

where $\alpha(x,t)$ and $\alpha(\tilde{x},\tilde{t})$ are the values of α at positions x and $\tilde{x}$, respectively, and $\langle\alpha\rangle$ is the average over all x and t. The time averaging $\langle\ \rangle$ has been done for 10^6 time steps ($dt = 0.001$) and the point chosen is $\tilde{x} = \frac{L}{2}$ ($L = 1000; dx = 0.10$). The rapid loss of spatial correlation function indicating the occurrence of spatiotemporal chaos is observed for $\sigma < \sigma_{AC}$ shown in Sec. IV B. The numerically determined largest Lyapunov exponent is $\mathcal{A}_{\max} = 0.05$ for the parameter set $\mu = 155.0$, $\phi = 5.20$, confirming the existence of spatiotemporal chaos in the system.

B. Spatiotemporal dynamics: In the presence of flow ($\sigma \neq 0$)

To proceed further, we set the system parameters ($\mu = 155, \phi = 5.2$) such that the system without flow admits spatiotemporal chaos [Fig. 4(a)]. Now we gradually increase the value of the dimensionless velocity σ to study the effect of advection on a system characterized by wave-induced spatiotemporal chaos. To start with, the value of the flow is well below the critical curve for transition from absolute

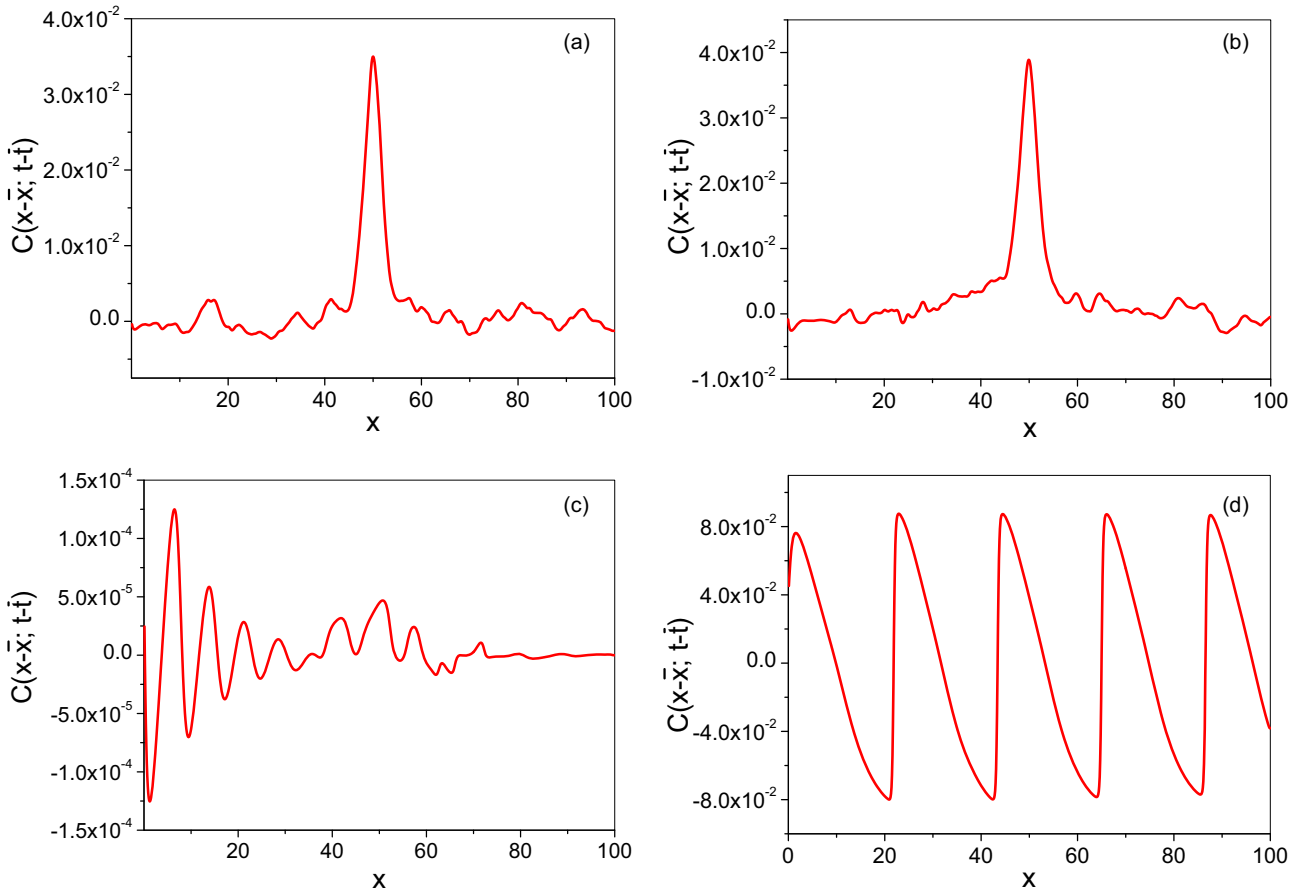

FIG. 6. (Color online) Spatial correlation functions for the system corresponding to space-time plots in [Figs. 4(a)–4(d)]: (a) absolute instability region, (b) absolute instability region, (c) convective instability region, and (d) stationary pattern region. Parameter set: $\mu = 155$ and $\phi = 5.20$.

to convective instability (σ_{AC}), and the system continues to show spatiotemporal chaos [Fig. 4(b)]. For flow values above σ_{AC}, the systems enter the zone of convective instability and the corresponding space-time plot depicts such a change [Fig. 4(c)]. On further increasing the flow velocity above the critical velocity (σ_s), the system makes a transition to a stationary patterned state [Fig. 4(d)]. The effect of the dimensionless flow (σ) has been monitored by observing the sign of the largest Lyapunov exponent ($\mathcal{A}_{\max}$) with the change in the strength of the advective flow. From Fig. 5 it is evident that the system ceases to admit the spatiotemporally chaotic dynamics for advection strengths $\sigma > \sigma_{AC}$ corresponding to change of sign of $\mathcal{A}_{\max}$ from positive to negative. The numerically obtained critical value of flow $\sigma_{AC} = 1.49$ is in good agreement with the σ_{AC} value calculated using Eq. (3.11). The spatial correlation functions for the system are shown in Figs. 6(a)–6(d) and correspond to the space-time plots of α for the different flow strengths depicted in Figs. 4(a)–4(d).

V. CONCLUSION

We have considered the two-variable Gray-Scott autocatalytic model in one dimension with equal diffusivities in a parameter space characterized by wave-induced spatiotemporal chaos. Again, since an open system entails advection, we have modeled our system using a reaction-diffusion-advection model to account for the flow. Linear stability analysis of the unstable focus has revealed that for a particular choice of flow velocity, transition from absolute to convective instability and subsequently to stationary patterns can be affected. Using this protocol we have been able to arrest wave-induced spatiotemporal chaos, as is evident from the space-time plots of the spatiotemporal α variable [Figs. 4(a)–4(c)], and the change in sign of the largest Lyapunov exponent $\mathcal{A}_{\max}$ as determined from the numerical simulations. Additionally, on increasing the flow above a second critical value we were able to realize a state characterized by stationary patterns [Fig. 4(d)]. The mechanism corresponding to the crossover from spatiotemporal chaos to stationary patterns is described by two successive transitions—one pertaining to a transition from absolute to convective instability and the other pertaining to the eventual flow-induced transition to a stationary patterned state. Thus, we have shown that by proper tuning of the velocity of the flow stream one can control and select different spatiotemporal regimes. Previous studies of reaction-diffusion-advection systems have focused on the transition to spatially inhomogeneous structures (patterns) in a mixed flow with temporally chaotic evolution of concentrations [28], which is distinctly different from the study presented in this paper. Possible experimental verification of this theoretical study can be sought by using a setup similar to the Couette reactor [21–23], as mentioned in the Introduction. Although the present paper deals exclusively with advective flow, one can devise similar control strategies by incorporating electric field [29] as an advective term for concerned spatially extended systems. The fact that advection can drastically change the stability properties of spatially extended systems is central to its use in directing the system [30–32] to a desired dynamical scenario [27].

ACKNOWLEDGMENT

D.D. would like to thank Prof. Deb Shankar Ray for useful discussions and a thorough reading of the manuscript. Thanks are due to the Council of Scientific and Industrial Research, Government of India, for partial financial support.

[1] S. H. Strogatz, *Nonlinear Dynamics and Chaos: With Applications to Physics, Biology, Chemistry, and Engineering* (Westview Press, Boulder, CO, 2014).
[2] I. R. Epstein and J. A. Pojman, *An Introduction to Nonlinear Chemical Dynamics: Oscillations, Waves, Patterns, and Chaos*, Topics in Physical Chemistry (Oxford University Press, New York, 1998).
[3] A. M. Turing, Philos. Trans. R. Soc. London B **237**, 37 (1952).
[4] A. B. Rovinsky and M. Menzinger, Phys. Rev. Lett. **69**, 1193 (1992).
[5] M. Kærn and M. Menzinger, Phys. Rev. E **60**, R3471 (1999).
[6] P. Andresén, M. Bache, E. Mosekilde, G. Dewel, and P. Borckmans, Phys. Rev. E **60**, 297 (1999).
[7] J. P. Eckmann, Rev. Mod. Phys. **53**, 643 (1981).
[8] J. H. Merkin, V. Petrov, S. K. Scott, and K. Showalter, Phys. Rev. Lett. **76**, 546 (1996).
[9] J. H. Merkin, V. Petrov, S. K. Scott, and K. Showalter, J. Chem. Soc., Faraday Trans. **92**, 2911 (1996).
[10] R. Wackerbauer and K. Showalter, Phys. Rev. Lett. **91**, 174103 (2003).
[11] Y. Nishiura and D. Ueyama, Physica D **150**, 137 (2001).
[12] S. Yonker and R. Wackerbauer, Phys. Rev. E **73**, 026218 (2006).
[13] M. Hildebrand, M. Bär, and M. Eiswirth, Phys. Rev. Lett. **75**, 1503 (1995).
[14] D. Krefting and C. Beta, Phys. Rev. E **81**, 036209 (2010).
[15] M. Bär and M. Eiswirth, Phys. Rev. E **48**, R1635(R) (1993).
[16] M. C. Cross and P. C. Hohenberg, Rev. Mod. Phys. **65**, 851 (1993).
[17] G. Benettin, L. Galgani, and J. M. Strelcyn, Phys. Rev. A **14**, 2338 (1976).
[18] A. Wolf, J. B. Swift, H. L. Swinney, and J. A. Vastano, Physica D **16**, 285 (1985).
[19] M. Kim, M. Bertram, M. Pollmann, A. V. Oertzen, A. S. Mikhailov, H. H. Rotermund, and G. Ertl, Science **292**, 1357 (2001).
[20] C. Beta, M. Bertram, A. S. Mikhailov, H. H. Rotermund, and G. Ertl, Phys. Rev. E **67**, 046224 (2003).
[21] W. Y. Tam, J. A. Vastano, H. L. Swinney, and W. Horsthemke, Phys. Rev. Lett. **61**, 2163 (1988).
[22] Q. Ouyang, J. Boissonade, J. C. Roux, and P. De Kepper, Phys. Lett. A **134**, 282 (1989).

[23] W. Y. Tam and H. L. Swinney, Physica D **46**, 10 (1990).
[24] J. R. Bamforth, S. Kalliadasis, J. H. Merkin, and S. K. Scott, Phys. Chem. Chem. Phys. **2**, 4013 (2000).
[25] P. Gray and S. K. Scott, Chem. Eng. Sci. **39**, 1087 (1984).
[26] P. A. Sturrock, Phys. Rev. **112**, 1488 (1958).
[27] P. Huerre, in *Propagation in Systems Far from Equilibrium* (Springer-Verlag, Berlin, 1987).
[28] A. V. Straube, M. Abel, and A. Pikovsky, Phys. Rev. Lett. **93**, 174501 (2004).
[29] S. Dutta and D. S. Ray, Phys. Rev. E **73**, 026210 (2006).
[30] P. N. McGraw and M. Menzinger, Phys. Rev. E **86**, 026208 (2012).
[31] G. G. Izús and A. D. Sánchez, Phys. Rev. E **88**, 062909 (2013).
[32] L. Stucchi and D. A. Vasquez, Phys. Rev. E **87**, 024902 (2013).